

Article

Phosphine Functionalization of GaAs(111)A Surfaces

Matthew C. Traub, Julie S. Biteen, David J. Michalak,
Lauren J. Webb, Bruce S. Brunschwig, and Nathan S. Lewis

J. Phys. Chem. C, **2008**, 112 (47), 18467-18473 • Publication Date (Web): 01 November 2008

Downloaded from <http://pubs.acs.org> on January 2, 2009

More About This Article

Additional resources and features associated with this article are available within the HTML version:

- Supporting Information
- Access to high resolution figures
- Links to articles and content related to this article
- Copyright permission to reproduce figures and/or text from this article

[View the Full Text HTML](#)

Phosphine Functionalization of GaAs(111)A Surfaces

Matthew C. Traub, Julie S. Biteen, David J. Michalak, Lauren J. Webb, Bruce S. Brunshwig,* and Nathan S. Lewis*

Beckman Institute and Kavli Nanoscience Institute, 210 Noyes Laboratory, 127-72, Division of Chemistry and Chemical Engineering, California Institute of Technology, Pasadena, California 91125

Received: May 6, 2008; Revised Manuscript Received: September 8, 2008

Phosphorus-functionalized GaAs surfaces have been prepared by exposure of Cl-terminated GaAs(111)A surfaces to triethylphosphine (PEt₃) or trichlorophosphine (PCl₃), or by the direct functionalization of the native-oxide terminated GaAs(111)A surface with PCl₃. The presence of phosphorus on each functionalized surface was confirmed by X-ray photoelectron spectroscopy. High-resolution, soft X-ray photoelectron spectroscopy was used to evaluate the As and Ga 3d regions of such surfaces. On PEt₃ treated surfaces, the Ga 3d spectra exhibited a bulk Ga peak as well as peaks that were shifted to 0.35, 0.92 and 1.86 eV higher binding energy. These peaks were assigned to residual Cl-terminated Ga surface sites, surficial Ga₂O and surficial Ga₂O₃, respectively. For PCl₃-treated surfaces, the Ga 3d spectra displayed peaks ascribable to bulk Ga(As), Ga₂O, and Ga₂O₃, as well as a peak shifted 0.30 eV to higher binding energy relative to the bulk signal. A peak corresponding to Ga(OH)₃, observed on the Cl-terminated surface, was absent from all of the phosphine-functionalized surfaces. After reaction of the Cl-terminated GaAs(111)A surface with PCl₃ or PEt₃, the As 3d spectral region was free of As oxides and As⁰. Although native oxide-terminated GaAs surfaces were free of As oxides after reaction with PCl₃, such surfaces contained detectable amounts of As⁰. Photoluminescence measurements indicated that phosphine-functionalized surfaces prepared from Cl-terminated GaAs(111)A surfaces had better electrical properties than the native-oxide capped GaAs(111)A surface, while the native-oxide covered surface treated with PCl₃ showed no enhancement in PL intensity.

I. Introduction

Surface passivation of semiconductors is increasingly critical as electronic devices shrink, and the surface-to-volume ratio increases accordingly. Silicon surfaces can be passivated by growth of a well-ordered thermal oxide layer. Although these thermal oxide layers are the dominant passivation method for industrial applications, the H-terminated Si(111) surface has been the subject of immense scrutiny as a platform for functionalization reactions of Si.^{1–4} For the Si(111) surface, passivation can be achieved through the formation of H-terminated interface, as produced by an aqueous fluoride etch.⁵ In addition to facilitating the direct attachment of a wide variety of chemical moieties,^{6–9} alkylation has produced long-lived chemical and electronic stability on the Si(111) surface.¹⁰

Gallium arsenide is an important material for many applications in modern semiconductor electronics.¹¹ A major barrier to even greater adoption of GaAs, particularly for solar energy conversion applications, is the cost and difficulty of providing effective surface passivation.¹² For most applications, an epitaxial capping layer, such as Al_xGa_{1-x}As, provides surface passivation and prevents the device performance from being dominated by surface-derived carrier trapping sites.^{13–15} The development of alternative, wet chemical methods for achieving effective passivation of GaAs surfaces could provide an attractive alternative to costly epitaxial growth methods for achieving control of the interfacial electronic properties of GaAs.

Previous research on chemical passivation of GaAs has largely focused on reactions of electron donor moieties with the (100) face of GaAs. Treatment of GaAs(100) with inorganic

sulfides has been shown to provide improved surface electrical properties.^{16–18} Similar effects have been observed with a variety of organic thiols,¹⁹ allowing formation of self-assembled monolayers on GaAs.^{20–22} More recently, hydrazine has been used to passivate GaAs with surficial Ga–N bonds, producing steady-state photoluminescence (PL) enhancements greater than those observed with sulfur-based treatments.²³ These chemical passivation techniques have also been shown to produce enhanced band gap emission from GaAs nanocrystals,²⁴ as well as single crystals. However, new surface functionalization reactions could provide the possibility of improved electronic or chemical stability or better compatibility with subsequent functionalization chemistry.

This work describes the reaction chemistry of phosphine reagents with the gallium-rich GaAs(111)A surface. This surface provides several potential advantages as a platform for GaAs functionalization chemistry. Dangling bonds on the GaAs(111)A face are oriented normal to the surface, allowing for better packing of surface functional groups. Furthermore, these dangling bonds are all associated with atop Ga atoms, allowing for more selective reaction of electron donor moieties with electrophilic surface sites. Finally, simple etching in HCl(aq) allows formation of a highly ordered,²⁵ chemically clean,²⁶ Cl-terminated GaAs(111)A surface, allowing functionalization reactions to proceed from an easily formed, well-defined starting surface. In contrast, the more widely studied GaAs(100) surface contains both Ga and As surface sites,²⁷ and aqueous etches have been shown to leave residual oxides and/or elemental As.^{28,29} Exploration of the fundamental chemical reactivity of the GaAs(111) surfaces may provide insight into new methods for passivation of single-crystal GaAs surfaces.

* To whom correspondence should be addressed. E-mail: nslewis@caltech.edu (N.S.L.).

Phosphines present a promising candidate for novel GaAs passivation chemistry. Phosphines contain a reactive electron lone pair on their central phosphorus atom, making them good donors for bonding to atop Ga sites on the GaAs(111)A surface. GaP is a wider band gap semiconductor than GaAs (2.26 vs 1.43 eV),³⁰ suggesting greater stability for Ga–P σ bonds than for GaAs bonds. Trioctylphosphine has been used as a passivating agent for the surfaces of II–VI nanocrystals, and has been noted to produce relatively high photoluminescence yields in such systems compared to other organic capping groups.³¹ A phosphine plasma has also been explored as a passivating agent for InGaAs.³² These results suggest an ability of basic P-containing reagents to effectively donate electron density to electrophilic Ga surface sites.

In this work, two phosphines, triethylphosphine (PEt₃) and trichlorophosphine (PCl₃), were chosen for reaction with the Cl-terminated GaAs(111)A surface. Both of these phosphines are liquids at room temperature and are well suited to solution functionalization reactions. While these groups are too large to pack onto every atop Ga site on the GaAs(111)A surface, these moieties are significantly smaller than more sterically constrained groups such as trioctylphosphine, and thus should enable a higher percentage of surface sites to be capped. These surface groups also provide an interesting contrast in reactivity, because the Cl groups on PCl₃ are relatively labile and easy to displace, allowing a variety of reactions and binding modes, whereas the ethyl groups on PEt₃ are relatively unreactive, and only reactions through the P lone pair should be possible. Finally, because PCl₃ is highly reactive, it may remove surface contaminants introduced after etching. This reactivity also allows direct reactions between PCl₃ and oxide-terminated GaAs without an aqueous etching step. Experiments on phosphine functionalized surfaces will provide data that complement previous passivation studies with sulfur and nitrogen moieties, and will address how potential trap-state contaminants are removed during the chemical functionalization process.

II. Experimental Procedures

A. Materials and Methods. For X-ray photoelectron spectroscopic (XPS) and soft X-ray photoelectron spectroscopic (SXPS) experiments, n-type, 325 μm thick GaAs(111) wafers, doped with Si to a carrier concentration of $1.7 \times 10^{18} \text{ cm}^{-3}$ and polished on the (111)A face, were acquired from AXT (Fremont, CA). Photoluminescence (PL) experiments were performed on undoped GaAs(111) wafers acquired from Atomergic (Farmingdale, NY). All solvents and chemicals used for surface functionalization were used as received from Aldrich Chemical Corp. All H₂O was obtained from a Barnsted Nanopure system and had a resistivity $>17.8 \text{ M}\Omega \text{ cm}$.

Prior to performing any surface chemistry, all of the GaAs samples were cleaned and degreased with successive rinses in H₂O, CH₃OH, acetone, 1,1,1-trichloroethane (TCE) or hexanes, acetone, CH₃OH, and H₂O. Samples were then etched in a 1:1 (v/v) mixture of concentrated HCl:H₂O at room temperature for 30 min, and were dried under a stream of N₂(g) without a water rinse. The samples were then placed into the antechamber of a N₂(g)-purged glovebox. Functionalization reactions were performed by immersing the samples in either neat PCl₃ (Aldrich) or in a 1.0 M solution of PEt₃ in tetrahydrofuran (THF) (Aldrich). For selected experiments, samples were introduced into the glovebox antechamber without etching in HCl(aq). All reactions were conducted for 3 h at ambient temperature. Samples were then removed from solution, rinsed with anhydrous THF (Aldrich), and dried under a stream of N₂(g).

B. Instrumentation. 1. XPS Measurements. Phosphine-functionalized samples used in the laboratory-based XPS experiments were introduced directly from the inert atmosphere glovebox to the antechamber of the XPS instrumentation, without deliberate exposure of the sample to ambient air. For SXPS measurements, the GaAs samples were functionalized in a glovebox and were then transported in vials that had been sealed under inert atmosphere to beamline U4A at the National Synchrotron Light Source (NSLS) at Brookhaven National Laboratory. The samples were then loaded, in air, into the SXPS antechamber, thus exposing these functionalized surfaces for several min to ambient air.

XPS and SXPS data were collected and analyzed using procedures described previously.^{26,33} XPS data were collected on a laboratory spectrometer with Al K α irradiation, while SXPS data were collected at the NSLS. For SXPS experiments, samples were illuminated at an incident energy of 90 eV, and the emitted photoelectrons were collected at normal to the sample surface by a VSW 100 mm hemispherical analyzer that was fixed at 45° off of the axis of the photon source. All energies are reported herein as binding energies in eV (eV). The intensities of the XPS data are given in arbitrary units. The sensitivity factors for the XPS experiments were obtained from the ESCA 2000 software package.

A detailed description of the techniques used for data analysis has been reported previously.²⁶ Briefly, the escape depths (i.e., the inelastic mean free paths) for the samples were calculated using the empirical method of Seah.³⁴ A Shirley background was calculated and subtracted from the original spectra.^{35–37} A least-squares method was then used to fit the spectra to a series of Voigt functions. The As 3d and Ga 3d SXPS spectra were fitted to a series of doublets, to account for the 3d_{5/2} and 3d_{3/2} components of each peak. The peaks that comprised each As 3d doublet were mutually constrained to have the same peak width, to be separated by $0.70 \pm 0.01 \text{ eV}$, and to have an area ratio of $(1:0.667) \pm 0.01$.³⁸ A similar procedure was used for the Ga peaks, except that the energy separation between the 3d_{5/2} and 3d_{3/2} peaks was set to $(0.44 \pm 0.01) \text{ eV}$.³⁸ Binding energies for all spectra were referenced to the As 3d_{5/2} peak of GaAs, whose binding energy was taken to be 41.1 eV.

2. Photoluminescence Measurements. For photoluminescence measurements, GaAs samples were mounted vertically and were illuminated on their front face with a continuous HeCd laser operating at 30 mW at 442 nm. The photoluminescence was collected from the front face of the GaAs, and was focused through a monochromator into a dry ice-cooled photomultiplier tube detector (Hamamatsu R632-01) that had been connected to a chart recorder. Scattered laser light was filtered out using a long-pass filter with a cutoff wavelength of 845 nm. Peak intensities were evaluated based on the intensity of the emission at 874 nm.

III. Results

A. Cl-Terminated GaAs(111)A Exposed to PEt₃. 1. XPS Data. Figure 1 shows the P 2p region of a Cl-terminated GaAs(111)A surface after exposure to PEt₃. The binding energy of the P 2p_{3/2} component of the P 2p doublet was 132.8 eV.³⁹ Measurements were also made in the Cl 2p peak region, since Cl was still present on the surface after treatment with PEt₃. Integration of the areas of the P 2p_{3/2} and Cl 2p peaks and correction for their relative sensitivity factors (0.789 and 2.285) yielded a P/Cl ratio of 0.4. The lower binding energy edge of the As 3p_{3/2} peak at $\sim 141 \text{ eV}$ ⁴⁰ is also visible in the P 2p spectra.

For some samples, the P 2p peak was best fit by two spin–orbit doublets, representing distinct chemical species on

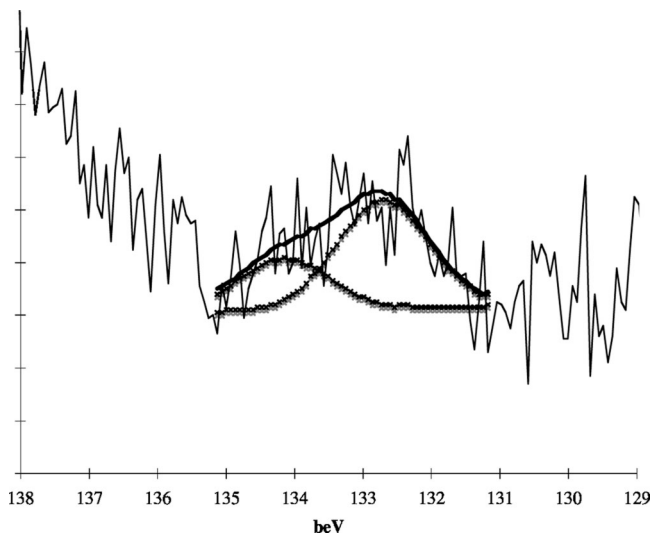


Figure 1. XPS data for the P 2p region of PET₃-functionalized surfaces. The low binding energy edge of the As 3p peak is also visible.

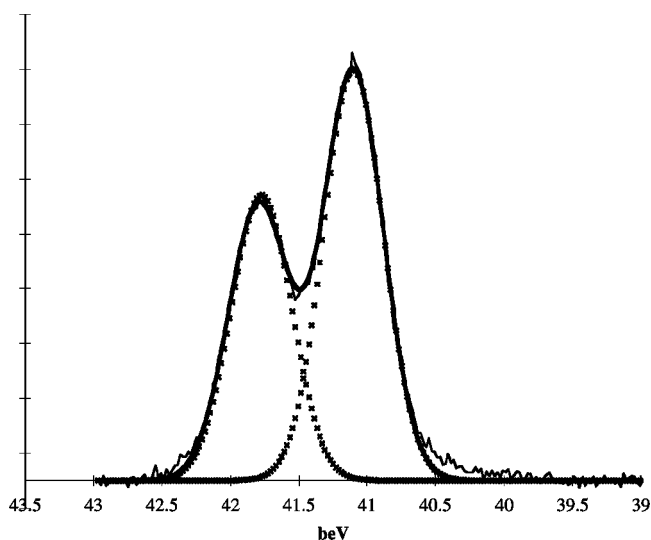


Figure 2. High-resolution SXPS As 3d data of PET₃-functionalized GaAs(111)A, fit to a single spin-orbit doublet.

the surface. In these instances, the lower binding energy peak displayed binding energies, P/Cl ratios, and surface coverages consistent with those described above. The higher binding energy 2p_{3/2} signal was centered at 133.8 eV, and was typically more intense than the lower binding energy peak.

The Ga and As 3d photoelectron peaks on the PET₃-treated GaAs(111)A surface appeared identical to those on the Cl-terminated GaAs(111)A surface.²⁶ The Ga 3d region was well fit to a single peak representing bulk Ga(As), while the As 3d region was well fit to a single spin-orbit doublet representing bulk (Ga)As. Both regions were free of oxides and other contaminants, to within the resolution of the experiment. Survey scans revealed the presence of adventitious carbon and oxygen species, but no other chemical species.

2. SXPS Data. The high-resolution SXPS As 3d data of PET₃-functionalized GaAs(111)A surfaces were well fit by a single spin-orbit doublet (Figure 2). A small amount of As₂O₃ was also observed at a binding energy of ~44.2 eV. This peak was too small and broad to obtain a reliable Shirley background or to make a quantitative evaluation of the surface coverage.

The high-resolution SXPS Ga 3d data of the PET₃-treated GaAs(111)A exhibited multiple peaks. Because the binding

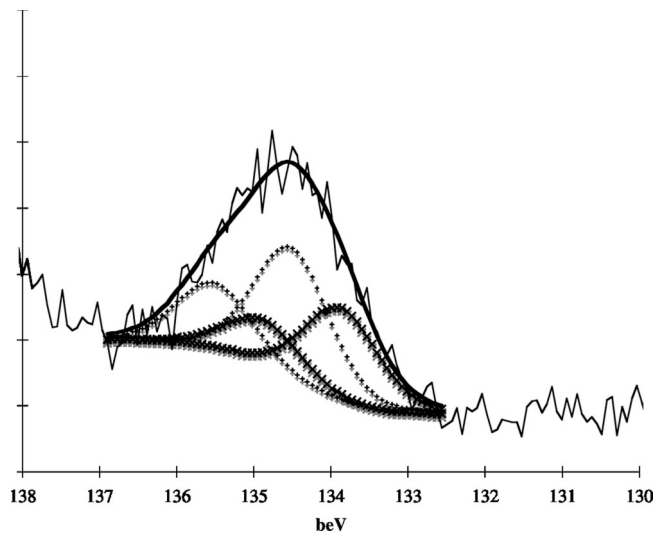


Figure 3. P 2p XPS data for Cl-terminated GaAs(111)A after reaction with PCl₃. The peak is better fit to two spin-orbit doublets, whose characteristics are described in the text.

energies of the relevant chemical species are more closely spaced²⁶ and the spacing between the spin-orbit doublet peaks is significantly smaller (0.44 eV vs 0.70 eV) for Ga 3d than for As 3d,³⁸ resolution of more than two chemical species in the Ga 3d SXPS data was difficult.

B. PCl₃ on Cl-Terminated GaAs(111)A. 1. XPS Data. The reaction chemistry of PCl₃ with Cl-terminated GaAs(111)A was complex. After treatment with PCl₃, a P 2p peak clearly appeared in the XPS data (Figure 3) while a Cl 2p peak was still present, with a P/Cl ratio of ~1.5:1. Fitting the P 2p signal to a single doublet yielded peak widths larger than those observed for PET₃-treated GaAs(111)A, so the P 2p signal was fit to two peaks. The P 2p_{3/2} component of the lower binding energy doublet was observed at 133.9 eV, while the P 2p_{3/2} component of the higher binding energy doublet was observed at 134.6 eV. The Ga and As peaks appeared free of contaminants in the XPS measurements.

2. SXPS Data. High-resolution SXPS data of the As 3d region of the PCl₃-treated GaAs(111)A surface confirmed that no As oxides or As⁰ were present at a detectable concentration. The observed signal was well fit to a single doublet. Similar to the Ga 3d spectra of the PET₃-treated surface (vide supra), the closer spacing of the Ga photoelectron peaks of the PCl₃-treated surface required more complicated processing for quantitative analysis. However, the raw spectra confirmed that these surfaces could be prepared with relatively minimal oxide contamination.

C. Native Oxide-Terminated GaAs(111)A Surfaces Exposed to PCl₃. 1. XPS Data. Native oxide-capped GaAs(111)A surfaces exposed to PCl₃ exhibited P 2p and Cl 2p XPS doublets (Figure 4). The relative surface abundance of P:Cl based on these peaks was 0.1–0.2, less than the value of 0.33 expected for simple atop binding of PCl₃. The 2p_{3/2} component of the P 2p doublet displayed a binding energy of 133.4 eV, slightly lower than the 133.9 eV binding energy observed for PCl₃ on etched GaAs(111)A surfaces.

Like the PET₃-treated etched GaAs(111)A surfaces, some of the PCl₃-treated oxide-capped GaAs(111)A surfaces showed broader, more intense P 2p peaks than other samples. These emissions were fit to 2 doublets, with P 2p_{3/2} components at 133.6 and 134.2 eV, respectively. In contrast to the PET₃-exposed GaAs(111)A surfaces, the intensity of both doublets of the PCl₃-treated, oxide-capped GaAs(111)A surfaces was enhanced, with

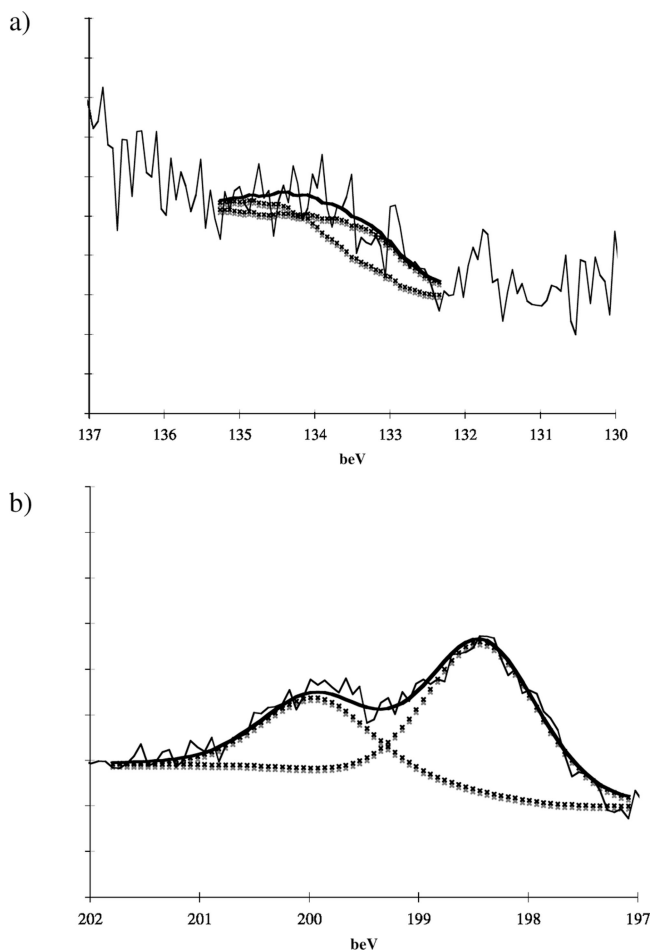


Figure 4. (a) The P 2p XPS peak of native oxide-capped GaAs(111)A surfaces after reaction with PCl_3 , fit to a single spin-orbit doublet. (b) The Cl 2p XPS spectra of this surface, as freshly prepared.

the lower binding energy component appearing significantly more abundant than Cl on the surface, having coverages in excess of 1 equivalent ML, based on the integrated Ga 3d and P 2p peak areas.

Several PCl_3 -exposed samples were annealed at 350 °C for 30 min at ~ 1 torr. Before annealing, the monolayer P coverage was 0.1–0.2 ML, as calculated using a previously published method.⁴¹ After the annealing step, the Cl XPS signal disappeared, and the intensity of the P increased, corresponding to a calculated coverage of 0.5–0.6 ML. However, the binding energy of the P 2p peak was unchanged. These observations suggest that the binding and integrity of the PCl_3 groups are extremely sensitive to trace levels of contaminants, and that loss of the Cl groups leads to drastic changes in the P 2p spectrum.

2. SXPS Data. SXPS data on the As 3d region indicated that PCl_3 was as effective at removing As oxide species as was an etch in $\text{HCl}(\text{aq})$. The Ga 3d signal showed slightly higher levels of contamination than was observed for $\text{HCl}(\text{aq})$ -etched surfaces, but was largely oxide-free. However, a detailed fit of the As 3d spectrum revealed an important difference between the PCl_3 -exposed and $\text{HCl}(\text{aq})$ -etched surfaces (Figure 5). The SXPS data on the PCl_3 -exposed surface were best fit with 2 doublets, one that represented a bulk component and smaller doublet that was shifted to 0.69 eV higher binding energy. This shift is consistent with the presence of elemental As on the PCl_3 -exposed oxide-capped GaAs(111)A surface. This higher energy foot was distinct from a small signal on the low-energy side of the As 3d peaks that was observed on all of the different functionalized

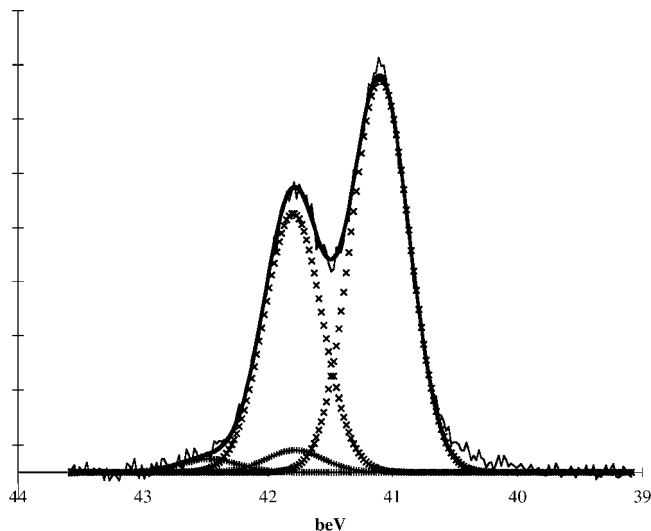


Figure 5. High-resolution SXPS As 3d spectrum of native oxide-capped GaAs(111)A after functionalization with PCl_3 . The spectrum is well fit by two spin-orbit doublets, representing bulk (Ga)As and shifted to 0.69 eV higher binding energy, As^0 .

surfaces. This apparent low-energy foot could not be well fit by additional peaks or by variations in peak shape.

D. Steady-State Photoluminescence Data. Steady-state PL data were obtained using undoped samples, to maximize the bulk emission efficiency.⁴² The intensity of the PL from native oxide-capped GaAs(111)A samples was taken as the reference level. A freshly $\text{HCl}(\text{aq})$ -etched GaAs(111)A surface yielded a factor of 2 increase in PL intensity relative to the native oxide-terminated GaAs(111)A surface, consistent with previous reports.²⁵ After treatment of the etched GaAs(111)A surface with PCl_3 , the PL was somewhat reduced, displaying an intensity 1.7 times greater than the reference oxide-capped GaAs(111)A sample. The PL of the improved samples gradually decayed after exposure to air, and after 36 h had reached the level of the native oxide-capped samples. In contrast, no increase in the PL intensity was observed for oxide-terminated GaAs(111)A surfaces that had not been etched but had instead been treated directly with PCl_3 . This behavior is consistent with the observation of As^0 on PCl_3 -treated oxide-capped GaAs(111)A surfaces.

IV. Discussion

To develop a more quantitative model for the binding of phosphine groups on the GaAs(111)A surface, equivalent monolayer coverages were calculated based on the P 2p and Ga 3d photoelectron peak areas measured on the XPS instrument. Based on a previously published model,⁴¹ the atomic size of P was calculated as 0.304 nm and the bulk density of P was taken as 1.823 g cm^{-3} . From this model, the P coverage for PET_3 -treated surfaces was 0.4 ± 0.1 ML, a value consistent with measurements of sterically constrained groups on the similarly spaced Si(111) surface.⁹ Combined with the observed P/Cl ratio of 0.4, the data indicate that 30–50% percent of the surface Ga sites are terminated by atop bound PET_3 , while the remaining Ga sites are Cl-terminated. The substitution of a neutral PET_3 surface-capping group for an anionic Cl^- group is probably facilitated by either a proton (supplied by an adsorbed hydrogen ion) or a solution impurity.

Consistent with the hypothesis that small amounts of impurities play a significant role in the observed results, the P 2p peak of some samples was best fit by two spin-orbit doublets, representing distinct chemical species on the surface. In these

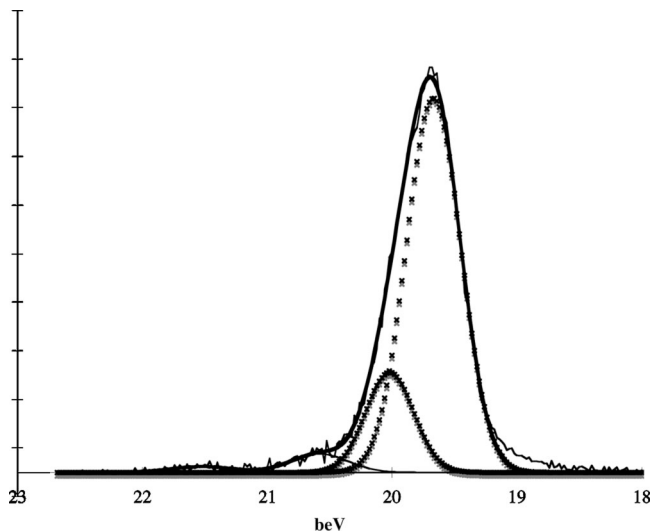


Figure 6. High-resolution SXPS Ga 3d spectrum of PEt₃-functionalized GaAs(111)A. The Ga 3d_{3/2} components of each peak have been deconvoluted from the spectrum and the data fit to a bulk Ga(As) peak, and peaks shifted 0.35, 0.92, and 1.86 eV to higher binding energy. These peaks correspond to Ga–Cl, Ga₂O, and Ga₂O₃, respectively.

instances, the lower binding energy peak displayed binding energies, P/Cl ratios, and surface coverages consistent with those described above. The 2p_{3/2} component of the second peak was centered at 133.8 eV, and was typically more intense, sometimes exhibiting surface coverages greater than 1 equivalent monolayer. This higher binding energy implies that oxidation of the P atom can be attributed to physisorption of an insoluble, oxidized phosphine species.

Because the binding energies of the relevant chemical species are more closely spaced for Ga 3d than for As 3d²⁶ and the spacing between the spin–orbit doublet peaks is significantly smaller (0.44 eV vs 0.70 eV),³⁸ resolution of the multiple peaks in the SXPS Ga 3d spectrum of the PEt₃ treated surfaces was facilitated by the subtraction of Ga 3d_{3/2} peak components. This procedure is well established for the analysis of Si 2p spectra.³³ For the purposes of this deconvolution, the height ratio and binding energy difference of the Ga 3d_{5/2} and Ga 3d_{3/2} peaks were fixed at the 0.667 and 0.44 eV respectively. Further, the fits obtained for these spectra depended strongly on the peak width constraints. Peak widths were therefore constrained to $\pm 10\%$ of the value observed for the bulk Ga(As) 3d_{5/2} peak on the Cl-terminated surface.²⁶

The deconvoluted Ga 3d spectra of the PEt₃-functionalized surface was well-fit by four Voigt function peaks (Figure 6). The second peak in the spectrum was shifted 0.35 eV to higher binding energy relative to the lowest energy bulk peak, consistent with the shift observed for Cl-bonded Ga surface sites. The next peak in the spectrum was shifted 0.92 eV to higher binding energy than the bulk peak, consistent with the 0.86 eV shift observed for Ga₂O on the native oxide-capped surface. The binding energy of the last peak on the surface was 1.86 eV higher than the bulk, a substantially larger shift than the 1.43 eV difference between the bulk and Ga₂O₃ peaks on the native oxide-capped surface. This discrepancy is likely due to the difficulty in fitting such a low intensity peak.

The absolute values of the corrected binding energies of these peaks were substantially (0.3 eV) higher than those observed on both the oxide and Cl-terminated surfaces. However, in the absence of an absolute charge reference, the binding energy shifts of surface species are more significant than their absolute

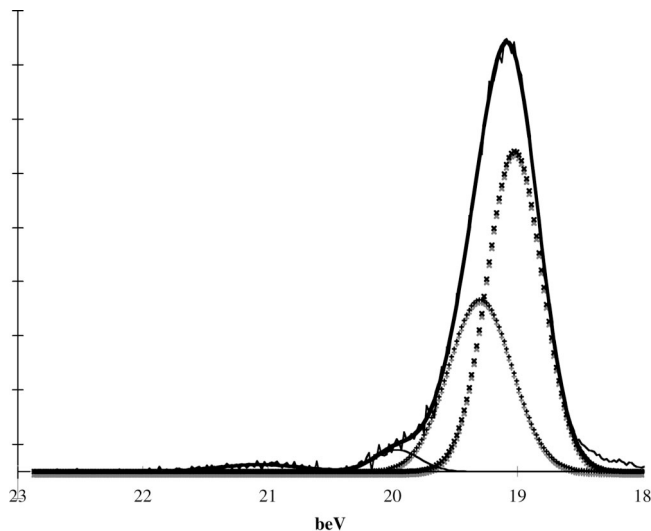


Figure 7. High-resolution SXPS Ga 3d spectrum of Cl-terminated GaAs(111)A after functionalization with PCl₃. The Ga 3d_{3/2} components of each peak have been deconvoluted from the spectrum and the data fit to a bulk Ga(As) peak, and peaks shifted 0.29, 0.92, and 2.04 eV to higher binding energy. The latter two peaks correspond to Ga₂O and Ga₂O₃, respectively, while the peak shifted by 0.29 eV has not been assigned.

values. Additionally, no discrete Ga–P bonding peak was assigned. Given that P is less electronegative than Cl and that the ethyl substituents are electron donating, it is likely that the PEt₃-capped Ga surface sites are more electron rich than Cl-capped sites, and hence their core level photoelectron peaks are shifted to a relatively lower binding energy. Due to this shift, any potential peak from these phosphine-capped species would be obscured by the bulk Ga(As) signal.

After applying the same deconvolution procedure to the SXPS spectrum of the Cl-terminated, PCl₃-treated surfaces, the data was fit to four peaks (Figure 7). These fits were quite sensitive to the initial conditions specified in the fitting procedure. To avoid selection bias in selecting a fit, the binding energies reported herein were averaged over multiple fits that were performed with different initial conditions. Thus, the standard deviations reported for these binding energy shifts reflect uncertainties in the fits rather than averages over multiple spectra.

The binding energy shift of 0.92 ± 0.03 eV between the bulk peak and the third peak is consistent with the value expected for Ga₂O, while the 2.04 ± 0.02 eV shift to the highest binding energy peak is similar to the value of 1.86 eV observed for higher order oxide contamination on the PEt₃ treated surface. The identity of the second peak in the spectrum is more difficult to ascertain. It is shifted to 0.29 ± 0.05 eV higher binding energy than the bulk peak. The upper range of this limit includes the shift of 0.34 eV observed for Ga–Cl bonds. However, as the loss of some Cl substituents from PCl₃ can be inferred from the observed P:Cl ratio, this peak may also represent different P bonding geometries, such as Ga–P multiple bonds, and no assignment can be conclusively made. Qualitatively though, it can be seen that these surfaces are prepared with extremely minimal oxide contamination.

Like the Ga 3d spectra described above, deconvolution of the Ga 3d_{3/2} peak components was required to obtain reasonable fits, and final values were sensitive to initial conditions. Although there was a small (0.2 eV) shift in the absolute binding energies observed, the Ga 3d spectrum was nearly identical to that observed for etched, PCl₃ treated surfaces. The spectrum

was fit to four peaks, corresponding to the bulk, Ga₂O, Ga₂O₃ and an unknown species shifted 0.30 eV to higher binding energy than the bulk.

Assignment of the SXPS As 3d_{5/2} peak shifted 0.69 eV from the bulk to As⁰ is confirmed by the failure of the PCl₃ treatment to improve the steady-state photoluminescence intensity of unetched samples. Elemental As is a well-known trap state for GaAs,^{43,44} and quantities of As⁰ sufficient to be observed by XPS will also be sufficient to quench carriers at the surface. Aqueous solutions may be necessary to convert surface As⁰ to As oxides, which can be dissolved away in the aqueous solution.⁴⁵ Aqueous rinsing has also been shown to significantly change the chemical composition of (NH₄)₂S functionalized GaAs surfaces.⁴⁶

An important unresolved question from these experiments is the binding mode of the PCl₃ on the Cl-terminated GaAs surface. The large excess of P relative to Cl on these surfaces, as well as the overall P coverage in excess of a monolayer for the etched surfaces, imply that simple atop binding of PCl₃ on Ga surface sites is not occurring. One possible mechanism is reaction of PCl₃ with surface bound water or hydroxides, forming surface bound phosphates. Alternatively, P may be incorporated into subsurface As sites, leaving a mixed GaAsP surface or separate Ga–P and As–P phases. Functionalization of GaAs(100) with (NH₄)₂S(aq) has been shown to produce separate Ga–S and As–S phases.⁴⁶ Additionally, shifts from As–S to Ga–S binding modes and changes in S coordination number have been observed at temperatures as low as 200 °C.⁴⁷

While the Ga 3d binding energies for Ga(P) and Ga(As) are essentially identical, the binding energy of the P 2p_{3/2} peak of GaP is known to occur at ~129 eV,^{48,49} while the value for PCl₃ has been reported to occur at 133.3 eV.⁵⁰ The observed shift to higher binding energies for PCl₃ on the Cl-terminated surface is more consistent with the formation of oxygen containing phosphorus species than the more reduced phosphides. In this model, a small fraction of the observed P is due to Ga-bonded P species, while a much greater fraction is due to these surface phosphates or phosphine oxides. This model is also consistent with the much lower phosphorus coverages observed for the reaction of PEt₃ with Cl-terminated surfaces, in which case the ethyl groups cannot be displaced to form phosphates.

V. Conclusions

The reaction chemistry of PEt₃ and PCl₃ with the GaAs(111)A surface has been characterized with X-ray photoelectron and soft X-ray photoelectron spectroscopy. Using the Cl-terminated GaAs(111)A surface as a starting point, PEt₃ has been found to react with 30–50% of surface sites, leaving Cl atoms bound to the remaining surface Ga atoms. This surface has a small amount of contamination from both Ga and As oxides, but is free of elemental As. The reaction of PCl₃ with the Cl-terminated surface leads to lower surface P coverages, closer to 20%. The surface-bound PCl₃ is more reactive than PEt₃, and significant displacement of the Cl ligands occurs. This surface is also nearly oxide free. The reaction of PCl₃ with the native oxide-terminated surface is similar, with nearly oxide-free surfaces observed. However, these surfaces contained small but observable concentrations of As⁰ and did not exhibit the steady-state photoluminescence enhancements observed on aqueously etched surfaces, and aqueous etching appears to be critical for removing impurities associated with electrical traps. These reactions are very sensitive to sample impurities and air oxidation. However, the ability to prepare phosphine terminated surfaces that are

initially free of oxide and As⁰ contaminants may provide a useful platform for further functionalization chemistry or as a precursor to UHV annealed surfaces with phosphorus based capping.

Acknowledgment. We gratefully acknowledge the Department of Energy, Office of Basic Energy Sciences, for support of this work. The research was carried out in part at the National Synchrotron Light Source, Brookhaven National Laboratory, which is supported by the U.S. Department of Energy, Division of Materials Sciences and Division of Chemical Sciences, under Contract No. DE-AC02-98CH10886. This research was carried out in part at the Molecular Materials Research Center of the Beckman Institute of the California Institute of Technology. We thank Michael Sullivan for use of the N₂(g)-purged glovebox at the NSLS.

References and Notes

- (1) Linford, M. R.; Fenter, P.; Eisenberger, P. M.; Chidsey, C. E. D. *J. Am. Chem. Soc.* **1995**, *117*, 3145.
- (2) Buriak, J. M.; Stewart, M. P.; Geders, T. W.; Allen, M. J.; Choi, H. C.; Smith, J.; Raftery, D.; Canham, L. T. *J. Am. Chem. Soc.* **1999**, *121*, 11491.
- (3) Bansal, A.; Li, X. L.; Lauer, I.; Lewis, N. S.; Yi, S. I.; Weinberg, W. H. *J. Am. Chem. Soc.* **1996**, *118*, 7225.
- (4) Bansal, A.; Li, X. L.; Yi, S. I.; Weinberg, W. H.; Lewis, N. S. *J. Phys. Chem. B* **2001**, *105*, 10266.
- (5) Yablonovitch, E.; Allara, D. L.; Chang, C. C.; Gmitter, T.; Bright, T. B. *Phys. Rev. Lett.* **1986**, *57*, 249.
- (6) Juang, A.; Scherman, O. A.; Grubbs, R. H.; Lewis, N. S. *Langmuir* **2001**, *17*, 1321.
- (7) Hurley, P. T.; Nemanick, E. J.; Brunschwig, B. S.; Lewis, N. S. *J. Am. Chem. Soc.* **2006**, *128*, 9990.
- (8) Bocking, T.; James, M.; Coster, H. G. L.; Chilcott, T. C.; Barrow, K. D. *Langmuir* **2004**, *20*, 9227.
- (9) Nemanick, E. J.; Hurley, P. T.; Brunschwig, B. S.; Lewis, N. S. *J. Phys. Chem. B* **2006**, *110*, 14800.
- (10) Webb, L. J.; Lewis, N. S. *J. Phys. Chem. B* **2003**, *107*, 5404.
- (11) Sze, S. M. *The Physics of Semiconductor Devices*, 2nd ed.; John Wiley and Sons: New York, 1981.
- (12) Gatos, H. C. *Surf. Sci.* **1994**, *300*, 1.
- (13) Ettenberg, M.; Kressel, H. *J. Appl. Phys.* **1976**, *47*, 1538.
- (14) Nelson, R. J.; Sobers, R. G. *J. Appl. Phys. Lett.* **1978**, *32*, 761.
- (15) Nelson, R. J.; Sobers, R. G. *J. Appl. Phys.* **1978**, *49*, 6103.
- (16) Skromme, B. J.; Sandroff, C. J.; Yablonovitch, E.; Gmitter, T. *Appl. Phys. Lett.* **1987**, *51*, 2022.
- (17) Yablonovitch, E.; Sandroff, C. J.; Bhat, R.; Gmitter, T. *Appl. Phys. Lett.* **1987**, *51*, 439.
- (18) Fan, J. F.; Oigawa, H.; Nannichi, Y. *Jpn. J. Appl. Phys. Part 2* **1988**, *27*, L2125.
- (19) Lunt, S. R.; Santangelo, P. G.; Lewis, N. S. *J. Vac. Sci. Technol. B* **1991**, *9*, 2333.
- (20) Adlkofer, K.; Tanaka, M.; Hillebrandt, H.; Wiegand, G.; Sackmann, E.; Bolom, T.; Deutschmann, R.; Abstreiter, G. *Appl. Phys. Lett.* **2000**, *76*, 3313.
- (21) Adlkofer, K.; Eck, W.; Grunze, M.; Tanaka, M. *J. Phys. Chem. B* **2003**, *107*, 587.
- (22) McGuinness, C. L.; Shaporenko, A.; Zharnikov, M.; Walker, A. V.; Allara, D. L. *J. Phys. Chem. C* **2007**, *111*, 4226.
- (23) Berkovits, V. L.; Ulin, V. P.; Losurdo, M.; Capezzuto, P.; Bruno, G.; Perna, G.; Capozzi, V. *Appl. Phys. Lett.* **2002**, *80*, 3739.
- (24) Traub, M. C.; Biteen, J. S.; Brunschwig, B. S.; Lewis, N. S. *J. Am. Chem. Soc.* **2008**, *130*, 955.
- (25) Lu, Z. H.; Chatenoud, F.; Dion, M. M.; Graham, M. J.; Ruda, H. E.; Koutzarov, I.; Liu, Q.; Mitchell, C. E. J.; Hill, I. G.; McLean, A. B. *Appl. Phys. Lett.* **1995**, *67*, 670.
- (26) Traub, M. C.; Biteen, J. S.; Michalak, D. J.; Webb, L. J.; Brunschwig, B. S.; Lewis, N. S. *J. Phys. Chem. B* **2006**, *110*, 15641.
- (27) Xue, Q. K.; Hashizume, T.; Sakurai, T. *Prog. Surf. Sci.* **1997**, *56*, 1.
- (28) Chang, C. C.; Citrin, P. H.; Schwartz, B. *J. Vac. Sci. Technol.* **1977**, *14*, 943.
- (29) Aspnes, D. E.; Studna, A. A. *Appl. Phys. Lett.* **1985**, *46*, 1071.
- (30) Lewis, N. S.; Rosenbluth, M. L. *Photocatalysis: Fundamentals and Applications*; Wiley-Interscience: New York, 1989.
- (31) Kalyuzhny, G.; Murray, R. W. *J. Phys. Chem. B* **2005**, *109*, 7012.
- (32) Sugino, T.; Sakamoto, Y.; Shirafuji, J. *J. Appl. Phys. Part 2* **1993**, *32*, L239.

- (33) Webb, L. J.; Nemanick, E. J.; Biteen, J. S.; Knapp, D. W.; Michalak, D. J.; Traub, M. C.; Chan, A. S. Y.; Brunshwig, B. S.; Lewis, N. S. *J. Phys. Chem. B* **2005**, *109*, 3930.
- (34) Seah, M. P. Quantification of AES and XPS. In *Practical Surface Analysis*, 2nd ed.; Briggs, D., Seah, M. P., Eds.; John Wiley and Sons: Chichester, 1990; Vol. Vol. 1, p 201.
- (35) Proctor, A.; Sherwood, P. M. A. *Anal. Chem.* **1982**, *54*, 13.
- (36) Shirley, D. A. *Phys. Rev. B* **1972**, *5*, 4709.
- (37) Contini, G.; Turchini, S. *Comput. Phys. Commun.* **1996**, *94*, 49.
- (38) Eastman, D. E.; Chiang, T. C.; Heimann, P.; Himpsel, F. J. *Phys. Rev. Lett.* **1980**, *45*, 656.
- (39) Error bars for XPS binding energies, determined from the spread of the fits over multiple samples, were $\sim \pm 0.1$ eV. Given the noise in the P 2p data, this may somewhat underestimate the error of these values. Further, in the absence of an absolute charging reference, the relative values are of more significance than the absolute binding energies.
- (40) Bahl, M. K.; Woodall, R. O.; Watson, R. L.; Irgolic, K. J. *J. Chem. Phys.* **1976**, *64*, 1210.
- (41) Haber, J. A.; Lewis, N. S. *J. Phys. Chem. B* **2002**, *106*, 3639.
- (42) Nelson, R. J. *J. Vac. Sci. Technol.* **1978**, *15*, 1475.
- (43) Woodall, J. M.; Freeouf, J. L. *J. Vac. Sci. Technol.* **1981**, *19*, 794.
- (44) Wieder, H. H. *J. Vac. Sci. Technol.* **1978**, *15*, 1498.
- (45) Kirchner, C.; George, M.; Stein, B.; Parak, W. J.; Gaub, H. E.; Seitz, M. *Adv. Funct. Mater.* **2002**, *12*, 266.
- (46) Lu, Z. H.; Graham, M. J.; Feng, X. H.; Yang, B. X. *Appl. Phys. Lett.* **1993**, *62*, 2932.
- (47) Scimeca, T.; Muramatsu, Y.; Oshima, M.; Oigawa, H.; Nannichi, Y. *Phys. Rev. B* **1991**, *44*, 12927.
- (48) Iwasaki, H.; Mizokawa, Y.; Nishitani, R.; Nakamura, S. *Surf. Sci.* **1979**, *86*, 811.
- (49) Franke, R.; Chasse, T.; Streubel, P.; Meisel, A. *J. Electron Spectrosc. Relat. Phenom.* **1991**, *56*, 381.
- (50) Fluck, E.; Weber, D. *Naturforsch. B* **1974**, *B 29*, 603.

JP803992H